Integrin and chemokine receptor gene expression in implant-adherent cells during early osseointegration

**Omar Omar · Maria Lennerås · Sara Svensson ·
Felicia Suska · Lena Emanuelsson · Jan Hall ·
Ulf Nannmark · Peter Thomsen**

Abstract The mechanisms of early cellular recruitment and interaction to titanium implants are not well understood. The aim of this study was to investigate the expression of pro-inflammatory cytokines, chemokines and adhesion markers during the first 24 h of implantation. Anodically oxidized and machined titanium implants were inserted in rat tibia. After 3, 12, and 24 h the implants were unscrewed and analyzed with quantitative polymerase chain reaction. Immunohistochemistry and scanning electron microscopy revealed different cell types, morphology and adhesion at the two implant surfaces. A greater amount of cells, as indicated by higher expression of small subunit ribosomal RNA (18S), was detected on the oxidized surface. Higher expression of CXC chemokine receptor-4 (at 12 h) and integrins, αv (at 12 h), $\beta 1$ (at 24 h) and $\beta 2$ (at 12 and 24 h) was detected at the oxidized surfaces. Significantly higher tumor necrosis factor-α (at 3 h) and interleukin-1β (at 24 h) expression was demonstrated for the machined surface. It is concluded that material surface properties rapidly modulate the expression of receptors important for the recruitment and adhesion of cells which are crucial for the inflammatory and regenerative processes at implant surfaces in vivo.

1 Introduction

The sequence of biological events following implantation of a material in vivo includes bleeding, inflammation and tissue regeneration [1, 2]. Whereas the molecular signals which are switched on and off after the encounter between single cell populations and specific material surface properties are becoming unraveled in vitro, the complex in vivo environment is largely unexplored. The rat tibia model has been used in several studies of early osseointegration [3–5]. In rat tibia, previous studies have demonstrated that the number of mesenchymal-like cells and the gene expression of markers of inflammation and bone remodeling are differently regulated at machined and anodically oxidized implants after 1 and 3 days [6]. Major unresolved questions are related to the chemotactic signals which promote the recruitment of inflammatory cells, osteogenic cells and their progenitors and how early differences in the properties of a material surface are sensed by cells in the in vivo environment.

Chemokines attract different cells depending upon which chemokines and/or chemokine receptors are expressed [7]. Further, chemokines are implicated in both inflammation and tissue repair [8, 9]. The chemokine receptor CXCR4 plays a critical role in homing and mobilization of different stem cell lineages [10–12] including MSCs [13–16]. This chemokine receptor

O. Omar (✉) · S. Svensson · F. Suska · L. Emanuelsson ·
P. Thomsen
Department of Biomaterials, Sahlgrenska Academy at University
of Gothenburg, Göteborg, Sweden
e-mail: omar.omar@biomaterials.gu.se

M. Lennerås
TATAA Biocenter AB, Göteborg, Sweden

J. Hall
Nobel Biocare AB, Göteborg, Sweden

U. Nannmark
Department of Medical Biochemistry and Cell Biology, Institute
of Biomedicine, Göteborg, Sweden

O. Omar · M. Lennerås · S. Svensson · F. Suska ·
L. Emanuelsson · P. Thomsen
BIOMATCELL VINN Excellence Center of Biomaterials
and Cell Therapy, Göteborg, Sweden

together with its unique ligand, stromal derived factor-alpha1 (SDF-α1), form an important axis determining the retention or migration of stem cells, either from the bone marrow to the injury site or visa versa. High binding of CXCR4 to SDF-α1 at the injury site ensure the retention of the mobilized CXCR4-positive cells in the repair process [17].

Monocyte chemoattractant protein-1 (MCP-1) (chemokine CCL2) is an important mediator for the recruitment of monocyte/macrophages [18–21]. High expression of MCP-1 was demonstrated in the response of human monocyte/macrophages [22] and osteoblasts [23] to titanium particles, respectively, in vitro. Interleukin-8 (IL-8), is a chemoattractant for neutrophils, and also has a wide range of pro-inflammatory effects that include stimulation of neutrophil degranulation and increased expression of cell adhesion molecules [24]. Its main receptor, IL-8R (also known as CXCR1) is the only IL-8 receptor expressed by neutrophils [25].

Attachment to a surface is a critical first step in the cell response to a biomaterial [26]. It signifies a fundamental cellular process, assumed to directly influence cell growth, differentiation and migration as well as tissue integrity and repair [27]. In vivo, the early cellular interaction to a biomaterial is mediated through a surface layer of proteins. It is via this protein rich layer that cells bind to surfaces using several families of adhesion receptors including heterodimeric molecules, the integrins. The cellular anchorage to the extracellular matrix proteins is linked to the cell interior by physically coupling the integrin receptors to the contractile cytoskeleton, mediated by focal adhesion proteins such as vinculin [28]. Cells of the osteoblastic linage predominantly express $\beta1$, $\alpha4$, $\alpha5$ and αv integrins in various combinations while the osteoclast cells exhibit higher levels of $\alpha v\beta3$ complexes in addition to $\beta1$ and $\alpha2$ heterodimers [27]. On the other hand, at least 13 integrins are expressed by leukocytes, among which the $\beta2$ is a unique leukocyte-specific integrin [29], with putative roles in leukocyte emigration, chemotaxis, phagocytosis, and other adhesion-dependent processes [30]. The $\beta2$ integrin has also been shown to be expressed by monocytes committed towards the osteoclast lineage [31].

The expression of integrins [27, 32–34] and the localization of vinculin [28, 35] on biomaterial surfaces has been largely studied in vitro. Results show that the expression of integrins and vinculin differs between materials depending on their surface topography and/or chemical composition. However, the role of surface properties on the gene expression of integrins and focal adhesion proteins has not been well described in vivo where the extracellular milieu is significantly different and the interaction with other cells and regulations by cytokines and growth factors may greatly influence the adhesion phenomenon.

The aims of the present in vivo study were: firstly, to determine if gene expression (qPCR) denoting inflammation was differently modulated at machined and oxidized titanium implants during the first 24 h of implantation, and, secondly to investigate the kinetics of early expression of markers for cellular chemotaxis and cell adhesion at the titanium implants.

2 Materials and methods

2.1 Implants

Screw-shaped titanium implants, 2 mm in diameter and 2.3 mm in length were used. Two types of surfaces were selected: machined and anodically oxidized (TiUnite^TM) surfaces (Nobel Biocare, Göteborg, Sweden), with surface roughness (Sa) of 0.3 μm and 1.2 μm, respectively, as measured by light interferometry (WYKO NT9100). The test implants were manufactured and sterilised by Nobel Biocare, Göteborg, Sweden.

2.2 The animal model

Experiments were performed according to the procedures described elsewhere [6]. In brief, fifteen female Sprague–Dawley rats underwent inhalation anaesthesia. The medial aspect of the proximal tibial metaphysis was exposed. Screw installation sites were prepared with ∅1.4, 1.6 and 1.8 mm round burs under profuse irrigation with NaCl 0.9%. Each rat received two oxidized implants in one tibia and two machined implants in the opposite tibia. The locations of implants were decided using a predetermined schedule, ensuring alteration between right and left legs. After surgery, the animals were allowed free postoperative movements with food and water ad libitum. The retrieval procedure was done at 3, 12 and 24 h (5 rats at each time point, two implants from each tibia) ($n = 10$). The rats were sacrificed and implants retrieved using a previously described RNA preserving protocol [6, 36]. In brief, rats received an intraperitoneal overdose of sodium pentobarbital (60 mg/ml) and implants were unscrewed with adherent biological material by a hexagonal screw driver and placed immediately in RNA preserving solutions for subsequent qPCR analysis. Additional four rats were used in order to study the distribution and morphology of the cells and tissue at the titanium implants using scanning electron microscopy (SEM) and immunohistochemistry. The animal experiments were approved by the University of Gothenburg Local Ethical Committee for Laboratory Animals (Dnr 306-2006).

2.3 Quantitative PCR

The procedure followed previously described detailed protocol [6]. Total RNA from each screw was extracted using RNeasy® Micro kit (QIAGEN GmbH, Hilden, Germany). Reverse transcription was carried out using iScript cDNA Synthesis Kit (Bio-Rad, Hercules, USA). Design of primers for TNF-α, IL-1β, IL-8R, MCP-1, CXCR4, integrins αv, β1, β2, β3 and vinculin, and 18S was performed using the Primer3 web-based software [37]. Assays were purchased from TATAA Biocenter AB, Göteborg, Sweden. Real-time PCR was performed in duplicates using the Mastercycler ep realplex (Eppendorf, Hamburg, Germany). Quantities of target genes were normalized using the expression of 18S ribosomal subunit. The normalized relative quantities were calculated using the delta Ct method and 90% PCR efficiency (k * 1.9$^{\Delta ct}$) [38].

2.4 Histology and immunohistochemistry

For histology and immunohistochemistry, two rats received oxidized and machined implants, one implant type in each tibia ($n = 2$). After anesthesia, the rats were fixated after 24 h of implantation by perfusion of modified Karnovsky media (2% paraformaldehyde, 2.5% glutaraldehyde in 0.05 M sodium cacodylate) (pH 7.4) via the left heart ventricle. The implant-bone specimens were post-fixated in modified Karnovsky media for 2 h, decalcified in 10% EDTA for 10 days and embedded in paraffin. While the paraffin was still in melting stage, the implants were unscrewed and the embedding procedure was continued. Ten µm sections were produced, mounted on glass slides and stained with hematoxylin and eosin for light microscopy (Nikon Eclipse E600). For immunostaining, 4 µm sections were produced, mounted on polylysine slides (Menzel GmbH and Co KG, Braunschweig, Germany), deparaffinized, hydrated and incubated with primary antibodies CD163 (sc-58965, Santa Cruz Biotechnology), a marker for monocyte/macrophage cells, and periostin (ab14041, Abcam, Cambridge, UK), a marker for mesenchymal stem cells and osteoprogenitors [39]. Negative control slides were prepared by omission of the primary antibody and incubation with 1% BSA in PBS.

2.5 Scanning electron microscopy

After fixation with modified Karnovsky, postfixation and decalcification, screws in bone-implant blocks retrieved after 1 days from 2 rats (2 specimens/implant type) were carefully removed, rinsed with sodium cacodylate buffer and impregnated with osmium using a modified osmium-thiocarbohydrazide-osmium technique (OTOTO). The specimens were then dehydrated in graded series of ethanol and dried with hexamethyldizilasane for 2×5 min. Specimens were mounted on stubs by means of carbon coated adhesive tape. In case of reduced conductivity, specimens were subjected to an additional sputter coat with palladium. All specimens were examined in a Zeiss DSM 982 Gemini scanning electron microscope.

2.6 Statistics

Analysis of the gene expression data was based on comparing the 18S-normalized relative expression of each gene at the two surfaces. For statistical comparisons, Wilcoxon signed rank test was used to analyze the differences in the gene expression levels between the two compared implant types at each specific time point. One way ANOVA followed by Dunnett T3 test was used to compare the gene expression levels between the three time points for a specific implant type. All statistical tests were done with SPSS® version 15.0 (SPSS Inc., Chicago, IL, USA). The level of confidence for either test was set to 95%, i.e. $P < 0.05$ was significant. The data presented in the graphs is mean ± SEM. The number of specimens used for gene expression analysis, histology, immunohistochemistry and scanning microscopy is given in Table 1.

3 Results

3.1 Gene expression analysis

Based on temporal expression at the three evaluation time points, the panel of gene markers was divided into three groups: chemotaxis (cell migration and homing) markers, pro-inflammatory markers and cell adhesion markers.

Table 1 Summarize the number of rats and implants used for each analytical technique

Type of analysis	Number of rats	Locations (right and left)	Number of implants (n)
qPCR	5 rats	2 implants per tibia	10 implants of each type
SEM	2 rats	1 implant per tibia	2 implants of each type
H and IHC	2 rats	1 implant per tibia	2 implants of each type

The gene expression analysis, using quantitative polymerase chain reaction (qPCR), was performed for three different time periods (3, 12 and 24 h). The morphological analyses, using scanning electron microscopy (SEM), histology (H) and immunohistochemistry (IHC), were performed for one time period (24 h)

3.1.1 18S ribosomal RNA expression

Higher level of 18S was associated with the oxidized compared to the machined surfaces at all tested time periods. The difference in 18S expression was statistically significant after 12 and 24 h (Fig. 1, Table 2). A continuous decrease of 18S expression level was observed for both surfaces with time.
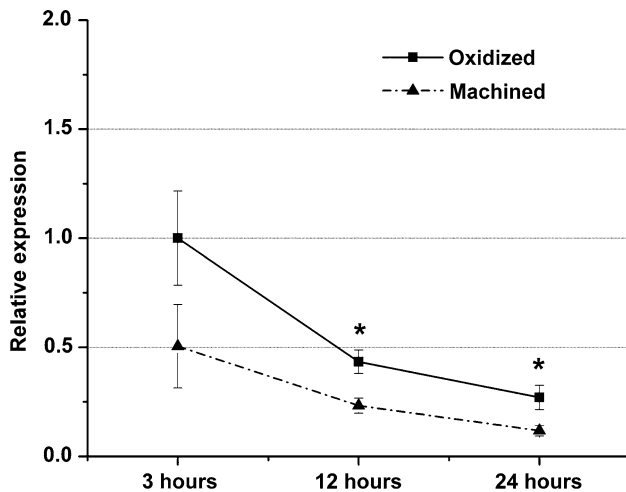
Fig. 1 Gene expression of 18S ribosomal subunits at oxidized and machined surfaces. The connecting line is only intended for visualization of the data series and does not suggest a trend. Statistically significant differences between the two surfaces are indicated in stars. The differences between the two tested implants were analyzed with Wilcoxon signed rank test. (* $P < 0.05$) $N = 10$ Mean ± SEM

Table 2 Results presented as the ratio between RNA expression in cells attached to oxidized implants ($n = 10$) and RNA expression in cells attached to machined implants ($n = 10$) after normalization to 18S

Gene marker	3 h	12 h	24 h
18S	1.98	1.87*	2.30*
IL-8R	0.76	1.28	1.20
MCP-1	0.71	1.37	0.49
CXCR4	1.11	11.87*	0.64
TNF-α	0.46*	1.00	0.55
IL-1β	0.62	1.37	0.35*
Integrin-αv	1.09	1.52*	0.64
Integrin-β1	1.28	1.03	2.16*
Integrin-β2	1.18	1.92*	2.08*
Integrin-β3	1.24	0.85	0.74
Vinculin	1.37	1.10	1.26

* $P < 0.05$

Values above 1 indicate more gene expression at the oxidized surfaces while values below 1 indicate more gene expression at the machined surfaces

3.1.2 Gene expression of chemotaxis markers

Neutrophils are one of the first cells that migrate to the site of inflammation. IL-8R (CXCR1) is an important key mediator involved in their recruitment. The gene expression profile of CXCR1 was determined at the interface of the two tested implant types. For both implant types, IL-8R expression showed a statistically significant increase from 3 h to 12 h and significantly decreased thereafter. No significant difference in the IL-8R expression level could be detected between the machined and oxidized implant at any of the evaluation time periods (Fig. 2a, Table 2).

After 24 h of implantation, a 2-fold higher expression level of MCP-1, a chemotactic factor for monocytes, was detected at the machined compared to the oxidized surfaces (Fig. 2b, Table 2). Oxidized implants showed a peak of MCP-1 expression after 12 h of implantation.
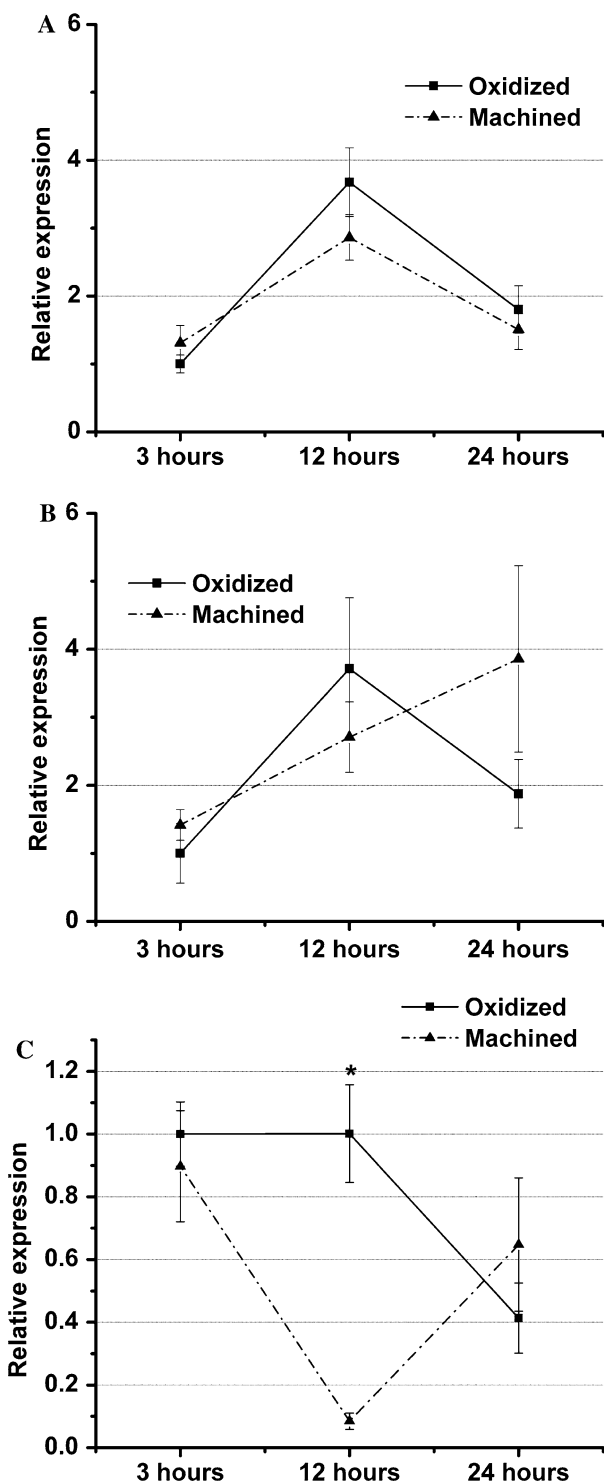
The expression of chemokine receptor CXCR4 was 11-fold significantly higher at the oxidized surfaces compared to the machined surfaces after 12 h of implantation (Fig. 2c, Table 2). From 3 h to 12 h, oxidized surface kept similar level of CXCR4 expression and thereafter decreased.

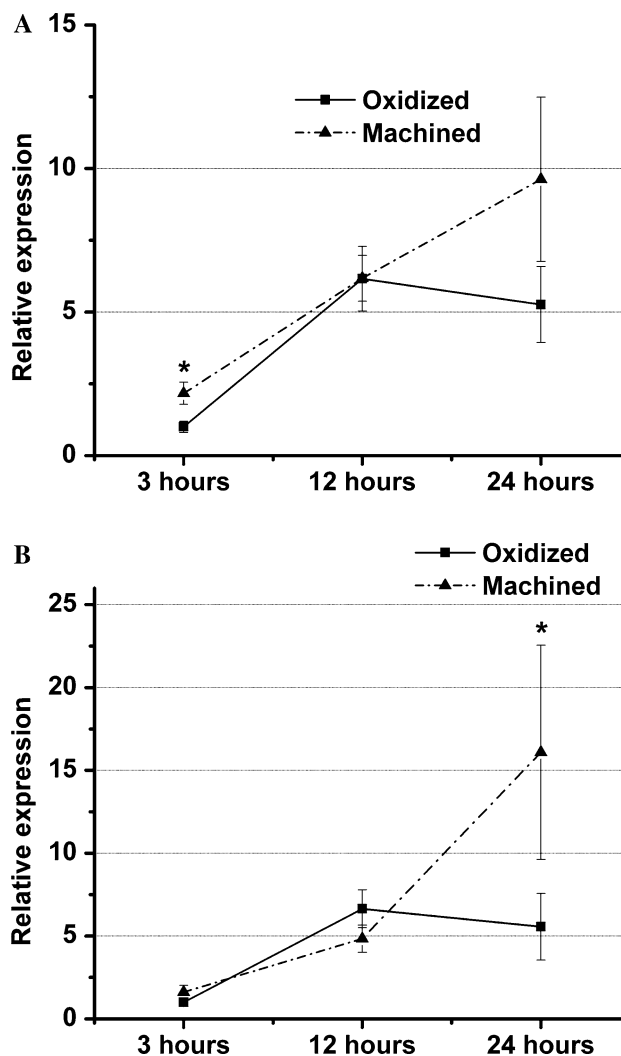### 3.1.3 Gene expression of pro-inflammatory markers

Compared to the oxidized ones, machined surfaces were associated with 2-fold higher expression of TNF-α after 3 and 24 h of implantation (Fig. 3a, Table 2). IL-1β was 3-fold significantly higher at the machined implants after 24 h of implantation (Fig. 3b, Table 2). Both cytokine expression levels were continuously increasing with time at the machined surfaces and had their peak after 24 of implantation. The expression levels of the two cytokines reached a peak at the oxidized implants after 12 h of implantation.

3.1.4 Gene expression of cell adhesion markers

After 12 h, the gene expression of αv integrin was 1.5-fold significantly higher at the oxidized implants than at the machined ones (Fig. 4a, Table 2). At 24 h, the pattern of αv integrin expression was reversed from that seen at 12 h. The reverse was indicated by 2-fold higher expression of αv integrin at the machined surfaces compared to the oxidized ones, although not statistically significant. On the contrary, the expression of integrin-β2 reserved a 2-fold significantly higher expression at the oxidized implants compared to the machined counterparts at 12 and 24 h (Fig. 4c, Table 2). At the 24 h time period, 2-fold significantly higher expression of integrin-β1 was observed at the oxidized implant compared to the machined ones (Fig. 4b, Table 2). Neither integrin-β3 (Fig. 4d, Table 2) nor vinculin (Table 2) showed any significant differences between the oxidized and machined surfaces at any of the evaluation periods.

Fig. 2 Gene expression of chemotaxis markers at oxidized and machined surfaces. **a** Interleukin-8R (IL-8R) gene expression. **b** Monocyte chemoattractant protein-1 (MCP-1) gene expression. **c** CXC chemokine Receptor-4 (CXCR4) gene expression. The connecting line is only intended for visualization of the data series and does not suggest a trend. Statistically significant differences between the two surfaces are indicated in stars. The differences between the two tested implants were analyzed with Wilcoxon signed rank test. (* $P < 0.05$) $N = 10$ Mean $\pm$ SEM


Fig. 3 Gene expression of pro-inflammatory markers at oxidized and machined surfaces. **a** Tumor necrosis factor-α (TNF-α) gene expression. **b** Interleukin-1β (IL-1β) gene expression. The connecting line is only intended for visualization of the data series and does not suggest a trend. Statistically significant differences between the two surfaces are indicated in stars. The differences between the two tested implants were analyzed with Wilcoxon signed rank test. (* $P < 0.05$) $N = 10$ Mean $\pm$ SEM

Temporally, machined implants showed peaks of β1, β2 and β3 integrin expression at 12 h of implantation. Integrin αv expression at the machined implants was constantly increasing with time and attained a peak after 24 h of implantation. The oxidized implants showed peaks of β1, β2 and αv integrins after 12 h of implantation. The highest expression of β3 integrin at the oxidized implants was observed after 3 h of implantation and decreased thereafter.
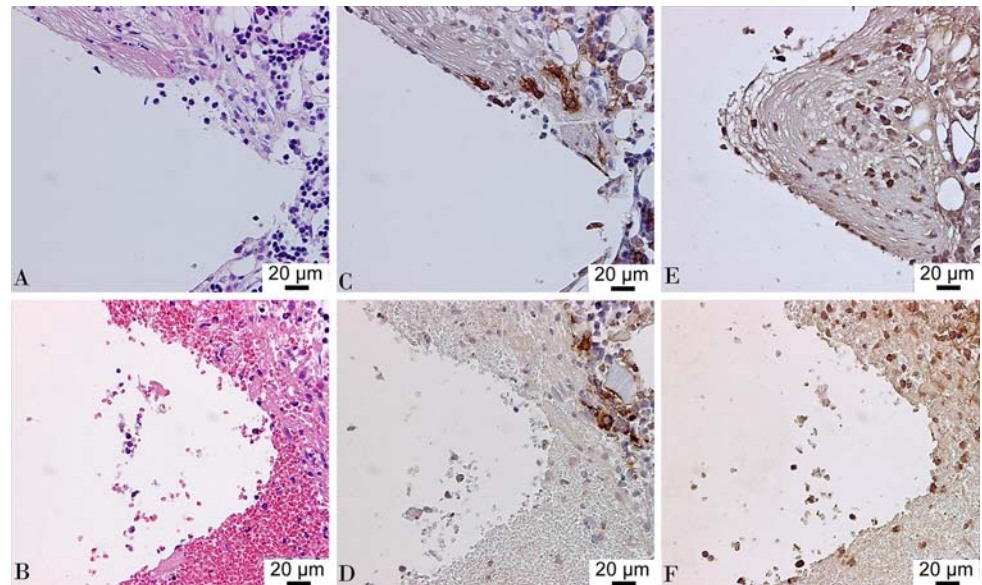
3.2 Immunohistochemical analysis

The H&E and the immunohistochemically stained sections revealed an early organization of blood hematoma within

Fig. 4 Gene expression of cell adhesion markers at oxidized and machined surfaces. Statistically significant differences between the two surfaces are indicated in stars. **a** integrin-αv gene expression. **b** integrin-β1 gene expression. **c** integrin-β2 gene expression. **d** integrin-β3 gene expression. The connecting line is only intended for visualization of the data series and does not suggest a trend. Statistically significant differences between the two surfaces are indicated in stars.The differences between the two tested implants were analyzed with Wilcoxon signed rank test. (* $P < 0.05$) $N = 10$ Mean ± SEM
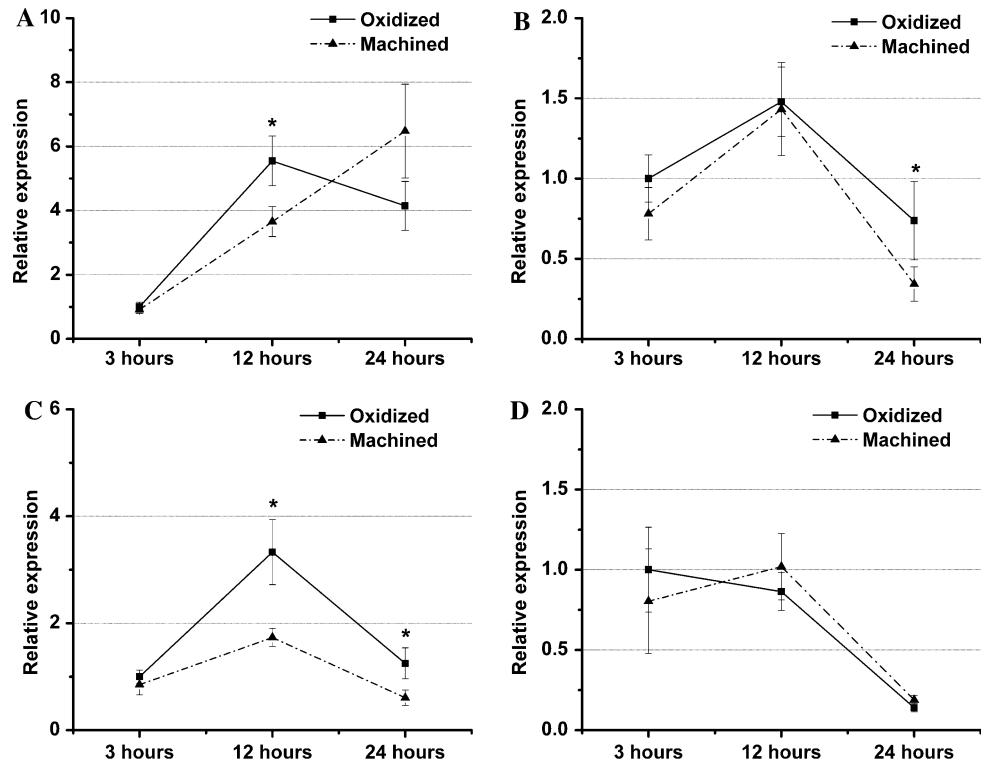
Fig. 5 Histological and immunohistochemical sections of the bone-implant interface after 24 h of implantation. The implants are removed. **a**, **b** Decalcified paraffin-embedded and H&E stained section for machined and oxidized titanium implants, respectively. **c**, **d** Immunolocalization of CD163-positive macrophages (MØ) at the machined and oxidized implants, respectively. **e**, **f** Immunolocalization of periostin-positive cells at the machined and oxidized implants, respectively. (Magnification × 40)


the threads of both implant types (Fig. 5). An interesting observation was that fibrin-like strands running parallel to the implant surface were prominently seen at the machined surfaces but not the oxidized ones. The immunohistochemical observations revealed that CD163 (a marker for monocytes and tissue macrophages) positive cells were scattered into the newly formed hematoma within the threads and at some locations very close to implant surface (Fig. 5c, d). Periostin (a marker for mesenchymal and osteoprogenitor cells) labeled cells were detected within the hematoma undergoing organization (Fig. 5e, f).

3.3 SEM analysis

A high proportion of fibrinous material adherent to the implant surfaces was revealed after removing the machined implants. Numerous erythrocytes and leukocytes were captured within the fibrin (Fig. 6). A similar picture was
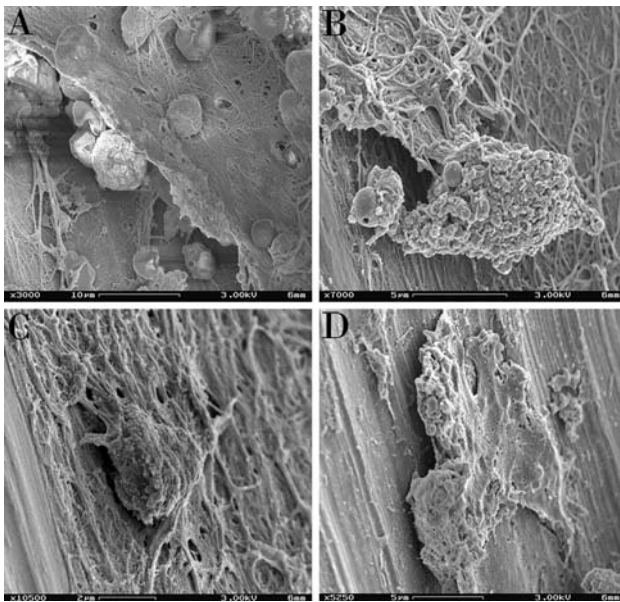
Fig. 6 SEM images of machined implant retrieved after 24 h. **a** Tissue surrounding the implant was loosely attached to the surface. Captured within this fibrin-like tissue were numerous erythrocytes and leukocytes (Magnification × 3,000). **b**, **c** Small size cells in range of 5-10 μm, probably leukocytes, entrapped within the fibrin strands (Magnifications × 7,000 and 10,500, respectively). **d** A mesenchymal-like cell is shown having a flat shape spreading out on the surface. The cellular processes do not show firm anchorage on the smooth surface (Magnification × 5,250)
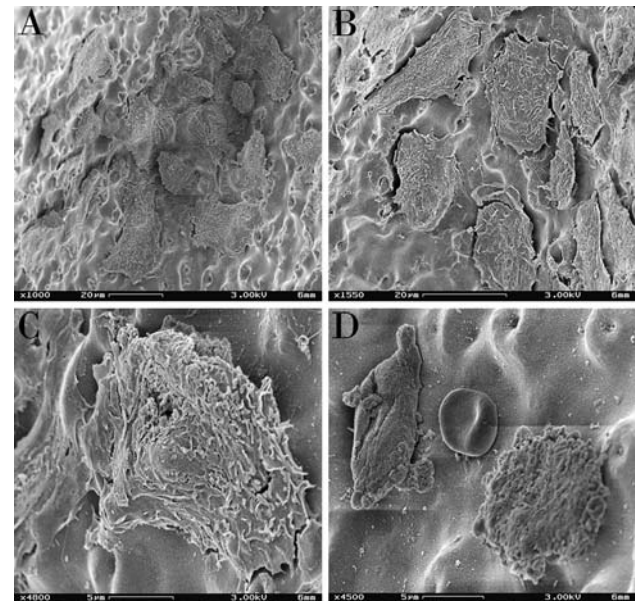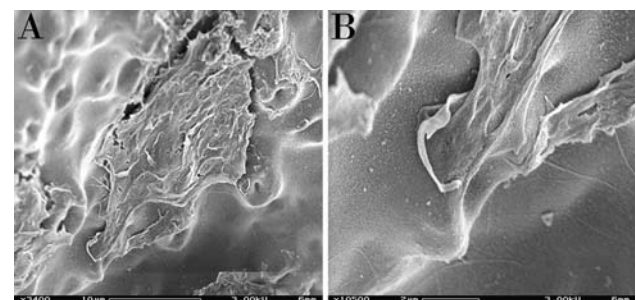

Fig. 7 SEM images of oxidized implant retrieved after 24 h. **a**, **b** Group of different size cells (5-30 μm in size) localized between the threads of the implants, the highest proportion of the cells is mainly at the bottom valley of the threads. The large cells (>15 μm) are mesenchymal-like cells (Magnification × 1,000 and 1,550, respectively). **c** On this surface the mesenchymal-like cell assumes a firm attachment to the surface. Cellular processes show an anchorage in the pores (<1 μm) of the surface (Magnification × 4,000). **d** Small size cells in range of 5-10 μm, most likely leukocytes, and an erythrocyte at the oxidized surface (Magnification × 4,500)

Fig. 8 SEM images of oxidized implant retrieved after 24 h. **a** Mesenchymal-like cell firmly attaching to the surface (Magnification × 3,400). **b** A higher magnification of the same cell in **a** showing the contact zone between extended cellular processes and a pore in the surface (<1 μm) (Magnification × 10,500)

not observed at the oxidized surfaces (Fig. 7). Depending on the size of the adherent cells, two different population of cells in addition to erythrocytes were roughly distinguished, large cells in range of 15–30 μm and smaller cells in range of 2–10 μm (Fig. 6a–d and 7a–d). The larger cells assumed to be mesenchymal-like cells or macrophages while the smaller cells are probably immune cells. Oxidized implants showed more mesenchymal-like cells attached over the surfaces with predominance at the bottom valley of the threads (Fig. 7a). Mesenchymal-like cells assumed more flat shape on the machined surfaces (Fig. 6d). An interesting observation was the firm anchorage of the mesenchymal-like cells on the oxidized implants by extending their processes onto the volcano-shaped pores (Fig. 8a, b).

4 Discussion

In the present study, the gene expression of pro-inflammatory cytokines, chemokines and adhesion molecules was elicited differently at titanium implants with different surface properties during the first 24 h of implantation. Machined implants induced nearly 2-fold higher expression of TNF-α (after 3 and 24 h), IL-1β, and MCP-1 (after

24 h). On the other hand, oxidized implants showed about 2-fold higher expression of integrins $\beta2$, αv (after 12 h) and $\beta1$ (after 24 h). Oxidized surfaces were also associated with 11-fold higher expression of CXCR4 (after 12 h). The results of the present study show that the prolonged signal of monocyte recruitment by the MCP-1 was coupled with delayed expression of pro-inflammatory cytokines at the machined implants. When this was corroborated with immunohistochemistry and SEM, at the 24 h, both

implants showed simultaneous presence of inflammatory and mesenchymal-like cells at their surfaces. However, two prominent features were differently observed between the two surfaces. The first was the predominance of mesenchymal-like cells with firm pseudopedic attachments to the oxidized surfaces. The second was the high prevalence of wide areas covered with fibrin-like tissue in association with leukocytes and erythrocytes at the machined surfaces but not at oxidized surfaces. Previous studies have shown the critical roles of fibrin (ogen) in mounting an inflammatory response at biomaterials in vivo [40–42]. Fibrinogen has been shown to activate NF-kB transcription factor [43, 44], increase expression and release of IL-1β [45] and decrease the alkaline phosphatase activity [46] in vitro. Moreover, a correlation between titanium surface texture and fibrin clot extension has been described in vitro [47]. Nevertheless, the mechanisms that regulate the fibrin organization and persistence on different titanium surfaces and the subsequent effect on the gene expression in vivo are unknown.

The exact role of the different surfaces in the diverse gene modulation is unknown. In the previous study [6], surface properties of the oxidized implants were listed with their possible effects on the expression of genes involved in the early inflammation and bone remodeling. Anodic oxidation process results in changed physico-chemical properties of the surface. Whereas a qualitative and quantitative data is available now regarding the chemistry, roughness, and oxide layer structure of the oxidized implants [48, 49], a little is known about their electric surface charge. The electric surface charge of a surface determines the zeta potential of that surface. Roesseler et al. found significant differences in the absolute zeta potentials for air formed and anodically formed oxide layers on titanium alloys [50]. Furthermore, other studies [51, 52] showed that thermal and chemical modification methods result in titanium dioxide with distinctly different zeta potentials. Several studies has pointed to the important role of the biomaterial zeta potential on the very early events such as the protein adsorption [51, 53], apatite formation [52], cell attachment [54], cell proliferation [51] and osteogenic gene expression [55, 56]. The hydroxide (–OH) content and crystalline structure of the surface layer were found to be important factors affecting the zeta potential. Higher levels of hydroxide groups [49] and crystalline structures [48] have been attributed to commercial oxidized implants. While this may indicates effect on the gene expression seen in this study, detailed experiments are needed, firstly to determine the precise zeta potential values of the current oxidized surfaces and secondly to evaluate their effects on the gene expression in the in vivo environment.

In contrast to many observations on the mid- and long-term responses to implants, less detailed information is available on the events taking place during the early hours after implantation in bone [57]. Soft tissue studies using titanium discs evaporated with differently functionalized gold layers showed differences in chemotactic response between the different functionalities after 24 h but not 3 h of implantation [58]. Using the same model, two other separate studies revealed higher release of TNF-α in response to porous titanium with and without plasma protein layer compared to machined titanium after 3 h [59], as well as for machined titanium compared to copper after 12 h [60]. In the latter study, IL-1β was significantly higher at the copper discs compared to titanium ones after 3, 12 and 48 h. While it is not known if similar inflammatory responses occur also in bone, the present data is in agreement with the soft tissue observations in the way that different surface properties induced different pro-inflammatory responses during the initial and early phase of implantation.

The mechanism of recruitment of different cell populations at the tissue-implant interface in bone is hitherto unknown. In the present study, expression markers for three different cell types were explored. IL-8R (CXCR1) expression, a marker for neutrophil recruitment, showed no significant difference between the two test implants. These results are consistent with the morphological observations showing no prevalence of neutrophils at one surface compared to the other. In conjunction with the transient nature of the neutrophils at the inflammation site, the temporal expression of IL-8R showed a peak after 12 h and declined thereafter at both implant surfaces. On the other hand, the high expression of MCP-1 (CCL2) in cells at the machined surfaces, simultaneously with a high expression of both TNF-α and IL-1β, indicates that machined surfaces promote an early and relatively stronger pro-inflammatory phase than the oxidized surface. This assumption is supported by analysis of gene expression at somewhat later time intervals (3 days and 6 days) using the same types of implants [6].

In the present study, the gene expression data in conjunction with qualitative histological, immunohistochemical and SEM preparations showed a predominance of mesenchymal-like cells on the oxidized surfaces during the first day of implantation. Similar observations were made after 3 days and 6 days [6]. The association between the strong influx of mesenchymal-like cells and subsequent bone formation at oxidized surfaces has been demonstrated by the observation of significantly higher alkaline phosphatase and osteocalcin expression at oxidized surfaces after 3 days and 6 days [6]. A key challenge is to determine the factors involved in the recruitment of the mesenchymal-like cells and the subsequent influence on bone formation at the implant site. In the current study and compared with machined surfaces, the cells at the oxidized

surface demonstrated an 11-fold higher expression of CXCR4 after 12 h, correlating to the predominance of MSCs observed at this surface. It has been shown that early peak expression of SDF-1α, the specific ligand for CXCR4, during the first day after tissue injury was associated with highest MSCs homed to injury site [61]. The important role of CXCR4-mediated SDF-1α recruitment of progenitor stem cells has previously also been demonstrated at injured sites in the heart [62], brain [63], and skin [17]. Further, a role has been implicated in ectopic bone formation [64] and bone injury [15]. In addition, in vitro experiments have shown that CXCR4 is involved in the migration of MSCs to gradients of chemotactic signals generated by cells obtained from site of tissue injury [65].

It can not be excluded that the significant difference of CXCR4 expression between the machined and oxidized titanium is due to a maximum relative expression by leukocytes. Recent observations have suggested a role of the CXCR4/SDF-1α axis in the removal and clearance of neutrophils from an injury site in order to promote the resolution of inflammation [66]. Having a short half life $\approx$ 6.5 h [66], senescent neutrophils show concomitant increase in CXCR4 expression [67] which directs their clearance and return toward the SDF-1α rich bone marrow [68]. However, the absence of any apparent differences between the two surfaces with respect to neutrophils, as indicated by similar IL-8R expression, SEM and histological observations, supports the assumption that the higher expression of CXCR4 at the oxidized surface is due to the higher prevalence of mesenchymal cells. Further studies are needed to explore the role and details of SDF-1α/CXCR4 axis in recruitment and maintenance of mesenchymal and inflammatory cells at bone-implant healing site.

Cells adhere to surfaces via integrins and the adherence is affected by the material surface properties [69]. This has particularly been demonstrated for substrate-cultured cells in vitro. In the present in vivo model, the expression of integrins αv, β2 (after 12 h) and β1 (after 24 h) was significantly increased at oxidized implants compared to machined ones. For both types of implants, all these integrins showed a peak at 12 h except for αv expression at the machined implants which peaked after 24 h. The integrin expression pattern of the adherent cells may reflect the temporal changes of the types and conformations of the target proteins adsorbed at the different surfaces. Previous in vitro observations on the stromal cell response to different proteins precoated on tissue culture plastics showed protein-specific expressions of β1, αv and β3 integrins [70]. Other in vitro data have shown that, among many upregulated integrins, β1 integrin was the integrin subunit with the greatest increase on a variety of substrates, compared with the level in cells prior to their addition to these

substrates [71]. Recent in vitro studies showed that the expression of β1 and β3 was upregulated after 21 days in osteoblast cell line cultured on titanium discs compared to tissue culture polystyrene whereas no differences were detected between oxidized and machined surfaces [72].

Acid etched titanium showed higher expression and peak of β1 and β3 integrins in the surrounding bone after 1 week compared to turned titanium and non implant defect [73]. Healing of bone defect was also associated with 1.5- and 2-fold higher expression of integrins β1 and β3, respectively, compared to the base-line expression and the expression was further increased by 3–7 fold after 2 weeks of placement of titanium implants [74]. While these in vivo observations are in line with our data in that β1 appears to be an important integrin upregulated during the healing phases of titanium implantation, the present data did not detect any difference in the expression of β3 between the two test implants. Furthermore, the present observation on modulation of integrin expression relies on the importance of analyzing the cells adherent to the implants rather than in the nearby bone tissue. However, the interpretation of in vivo integrin expression with respect to specific cell types should be under precaution, since different cell types and phenotypes share similar expression patterns of these heterodimeric complexes. In the present data the expression of β2 integrin, which has been shown to be specific for leukocytes [29] and not expressed by cells of osteoblastic linage [75], was higher at the oxidized implants. Integrin-β2 (CD11b/CD18) is also expressed by osteoclast progenitors [31]. The results from a previous study [6] showing a higher expression of osteoclastic marker (cathepsin K) at the oxidized surface suggest that the higher expression of β2 integrin seen in the present study is due to a higher osteoclastic differentiation.

Future studies may focus on the effect of each specific surface property on the regulation of gene expression in close vicinity to the implant surface. Furthermore, it is of great importance to analyze the biological components that might be implicated in the bone formation mechanisms at the interface, such as the Wnt signaling pathway. The determination of specific role of particular molecule or group of molecules in the osseointegration process may require the modulation of specific target genes by, for instance, the local application of specific growth factors or the employment of the knock-out or gene-deficient species. Currently, studies are being designed to combine the present model with other techniques. Some of these studies focus on the distinct proof and quantification of specific cellular subsets adherent to the retrieved implants. Other studies aim to find correlations between the early molecular response, dictated by gene expression analysis, and the kinetic changes in structure and stability of the interface. Furthermore, the clinical application of the sampling

procedure and the subsequent qPCR is currently being evaluated as a screening procedure for dental implants.

5 Conclusions

The results of the present experimental in vivo studies in rats demonstrate that implant surface properties influence protein-cell morphology, cell recruitment and gene expression at the immediate implant surface during the first 24 h after implant insertion in bone. Oxidized surfaces were associated with significantly higher expression of αv, $\beta 1$, and $\beta 2$ integrins, CXCR4 homing receptor, and number of recruited cells. Higher expression levels of proinflammatory cytokines tumor necrosis factor-α and interleukin-1β were attributed to machined implant surfaces. It is concluded that the present in vivo model allows detailed studies on the complex interplay between material surface properties, inflammatory cells, osteogenic cells and their progenitors.

References

1. Anderson J. Inflammation, wound healing and the foreign body response. In: Ratner B, Hoffman A, Schoen F, Lemons J, editors. Biomaterials science, an introduction to materials in medicine. San Diego: Academic Press; 1996. p. 165–73.
2. Thomsen P, Ericson L. Inflammatory cell response to bone implant surfaces. In: Davies JE, editor. The bone-biomaterial interface. Toronto: University of Toronto Press; 1991. p. 153–69.
3. Abron A, Hopfensperger M, Thompson J, Cooper LF. Evaluation of a predictive model for implant surface topography effects on early osseointegration in the rat tibia model. J Prosthet Dent. 2001;85:40–6.
4. Clokie CM, Warshawsky H. Morphologic and radioautographic studies of bone formation in relation to titanium implants using the rat tibia as a model. Int J Oral Maxillofac Implants. 1995;10:155–65.
5. Masuda T, Salvi GE, Offenbacher S, Felton DA, Cooper LF. Cell and matrix reactions at titanium implants in surgically prepared rat tibiae. Int J Oral Maxillofac Implants. 1997;12:472–85.
6. Omar O, Svensson S, Zoric N, Lennerås M, Suska F, Wigren S, et al. In vivo gene expression in response to anodically oxidized versus machined titanium implants. J Biomed Mater Res A. 2009. [Epub ahead of print]. doi:10.1002/jbm.a.32475.
7. Campbell DJ, Kim CH, Butcher EC. Chemokines in the systemic organization of immunity. Immunol Rev. 2003;195:58–71.
8. Amano H, Morimoto K, Senba M, Wang H, Ishida Y, Kumatori A, et al. Essential contribution of monocyte chemoattractant protein-1/C-C chemokine ligand-2 to resolution and repair processes in acute bacterial pneumonia. J Immunol. 2004;172:398–409.
9. Ringe J, Strassburg S, Neumann K, Endres M, Notter M, Burmester GR, et al. Towards in situ tissue repair: human mesenchymal stem cells express chemokine receptors CXCR1, CXCR2 and CCR2, and migrate upon stimulation with CXCL8 but not CCL2. J Cell Biochem. 2007;101:135–46.
10. Hoenig MR, Bianchi C, Sellke FW. Hypoxia inducible factor-1 alpha, endothelial progenitor cells, monocytes, cardiovascular risk, wound healing, cobalt and hydralazine: a unifying hypothesis. Curr Drug Targets. 2008;9:422–35.
11. Liao TS, Yurgelun MB, Chang SS, Zhang HZ, Murakami K, Blaine TA, et al. Recruitment of osteoclast precursors by stromal cell derived factor-1 (SDF-1) in giant cell tumor of bone. J Orthop Res. 2005;23:203–9.
12. Pitchford SC, Furze RC, Jones CP, Wengner AM, Rankin SM. Differential mobilization of subsets of progenitor cells from the bone marrow. Cell Stem Cell. 2009;4:62–72.
13. Dar A, Goichberg P, Shinder V, Kalinkovich A, Kollet O, Netzer N, et al. Chemokine receptor CXCR4-dependent internalization and resecretion of functional chemokine SDF-1 by bone marrow endothelial and stromal cells. Nat Immunol. 2005;6:1038–46.
14. Ji JF, He BP, Dheen ST, Tay SS. Interactions of chemokines and chemokine receptors mediate the migration of mesenchymal stem cells to the impaired site in the brain after hypoglossal nerve injury. Stem Cells. 2004;22:415–27.
15. Kitaori T, Ito H, Schwarz EM, Tsutsumi R, Yoshitomi H, Oishi S, et al. Stromal cell-derived factor 1/CXCR4 signaling is critical for the recruitment of mesenchymal stem cells to the fracture site during skeletal repair in a mouse model. Arthritis Rheum. 2009;60:813–23.
16. Wynn RF, Hart CA, Corradi-Perini C, O'Neill L, Evans CA, Wraith JE, et al. A small proportion of mesenchymal stem cells strongly expresses functionally active CXCR4 receptor capable of promoting migration to bone marrow. Blood. 2004;104:2643–5.
17. Ceradini DJ, Kulkarni AR, Callaghan MJ, Tepper OM, Bastidas N, Kleinman ME, et al. Progenitor cell trafficking is regulated by hypoxic gradients through HIF-1 induction of SDF-1. Nat Med. 2004;10:858–64.
18. Baggiolini M, Dewald B, Moser B. Human chemokines: an update. Annu Rev Immunol. 1997;15:675–705.
19. Graves DT, Jiang Y. Chemokines, a family of chemotactic cytokines. Crit Rev Oral Biol Med. 1995;6:109–18.
20. Graves DT, Jiang Y, Valente AJ. The expression of monocyte chemoattractant protein-1 and other chemokines by osteoblasts. Front Biosci. 1999;4:D571–80.
21. Rahimi P, Wang CY, Stashenko P, Lee SK, Lorenzo JA, Graves DT. Monocyte chemoattractant protein-1 expression and monocyte recruitment in osseous inflammation in the mouse. Endocrinology. 1995;136:2752–9.
22. Nakashima Y, Sun DH, Trindade MC, Chun LE, Song Y, Goodman SB, et al. Induction of macrophage C-C chemokine expression by titanium alloy and bone cement particles. J Bone Joint Surg Br. 1999;81:155–62.
23. Fritz EA, Glant TT, Vermes C, Jacobs JJ, Roebuck KA. Titanium particles induce the immediate early stress responsive chemokines IL-8 and MCP-1 in osteoblasts. J Orthop Res. 2002;20:490–8.
24. Videm V, Strand E. Changes in neutrophil surface-receptor expression after stimulation with FMLP, endotoxin, interleukin-8 and activated complement compared to degranulation. Scand J Immunol. 2004;59:25–33.
25. Murphy PM, Baggiolini M, Charo IF, Hebert CA, Horuk R, Matsushima K, et al. International union of pharmacology. XXII. Nomenclature for chemokine receptors. Pharmacol Rev. 2000;52:145–76.
26. Boyan B, Dean D, Lohmann C, Cochran D, Sylvia V, Schwartz Z. The titanium-bone cell interface in vitro: the role of the surface in promoting osteointegration. In: Brunette DM, Tengvall P,

Textor M, Thomsen P, editors. Titanium in medicine. New York: Springer; 2001. p. 561–85.

27. Sinha RK, Tuan RS. Regulation of human osteoblast integrin expression by orthopedic implant materials. Bone. 1996;18:451–7.

28. Diener A, Nebe B, Luthen F, Becker P, Beck U, Neumann HG, et al. Control of focal adhesion dynamics by material surface characteristics. Biomaterials. 2005;26:383–92.

29. Stewart M, Thiel M, Hogg N. Leukocyte integrins. Curr Opin Cell Biol. 1995;7:690–6.

30. Arnaout MA. Leukocyte adhesion molecules deficiency: its structural basis, pathophysiology and implications for modulating the inflammatory response. Immunol Rev. 1990;114:145–80.

31. Hayashi H, Nakahama K, Sato T, Tuchiya T, Asakawa Y, Maemura T, et al. The role of Mac-1 (CD11b/CD18) in osteoclast differentiation induced by receptor activator of nuclear factor-kappaB ligand. FEBS Lett. 2008;582:3243–8.

32. Krause A, Cowles EA, Gronowicz G. Integrin-mediated signaling in osteoblasts on titanium implant materials. J Biomed Mater Res. 2000;52:738–47.

33. Rouahi M, Champion E, Hardouin P, Anselme K. Quantitative kinetic analysis of gene expression during human osteoblastic adhesion on orthopaedic materials. Biomaterials. 2006;27: 2829–44.

34. ter Brugge PJ, Jansen JA. Initial interaction of rat bone marrow cells with non-coated and calcium phosphate coated titanium substrates. Biomaterials. 2002;23:3269–77.

35. Woodruff MA, Jones P, Farrar D, Grant DM, Scotchford CA. Human osteoblast cell spreading and vinculin expression upon biomaterial surfaces. J Mol Histol. 2007;38:491–9.

36. Omar O, Suska F, Lenneras M, Zoric N, Svensson S, Hall J, et al. The influence of bone type on the gene expression in normal bone and at the bone-implant interface: experiments in animal model. Clin Implant Dent Relat Res. 2009.

37. Rozen S, Skaletsky H. Primer3 on the WWW for general users and for biologist programmers. Methods Mol Biol. 2000;132: 365–86.

38. Pfaffl MW. A new mathematical model for relative quantification in real-time RT-PCR. Nucleic Acids Res. 2001;29:e45.

39. Coutu DL, Wu JH, Monette A, Rivard GE, Blostein MD, Galipeau J. Periostin, a member of a novel family of vitamin K-dependent proteins, is expressed by mesenchymal stromal cells. J Biol Chem. 2008;283:17991–8001.

40. Flick MJ, Du X, Witte DP, Jirouskova M, Soloviev DA, Busuttil SJ, et al. Leukocyte engagement of fibrin(ogen) via the integrin receptor alphaMbeta2/Mac-1 is critical for host inflammatory response in vivo. J Clin Invest. 2004;113:1596–606.

41. Hu WJ, Eaton JW, Ugarova TP, Tang L. Molecular basis of biomaterial-mediated foreign body reactions. Blood. 2001;98: 1231–8.

42. Tang L, Eaton JW. Fibrin(ogen) mediates acute inflammatory responses to biomaterials. J Exp Med. 1993;178:2147–56.

43. Rubel C, Gomez S, Fernandez GC, Isturiz MA, Caamano J, Palermo MS. Fibrinogen-CD11b/CD18 interaction activates the NF-kappa B pathway and delays apoptosis in human neutrophils. Eur J Immunol. 2003;33:1429–38.

44. Sitrin RG, Pan PM, Srikanth S, Todd RF III. Fibrinogen activates NF-kappa B transcription factors in mononuclear phagocytes. J Immunol. 1998;161:1462–70.

45. Cobb RR, Molony JL. Interleukin-1beta expression is induced by adherence and is enhanced by Fc-receptor binding to immune complex in THP-1 cells. FEBS Lett. 1996;394:241–6.

46. Nagao H. Fibrinogen affects blood and bone marrow cell functions on titanium in vitro. Kokubyo Gakkai Zasshi. 1998;65: 53–63.

47. Di Iorio D, Traini T, Degidi M, Caputi S, Neugebauer J, Piattelli A. Quantitative evaluation of the fibrin clot extension on different implant surfaces: an in vitro study. J Biomed Mater Res B Appl Biomater. 2005;74:636–42.

48. Jarmar T, Palmquist A, Branemark R, Hermansson L, Engqvist H, Thomsen P. Characterization of the surface properties of commercially available dental implants using scanning electron microscopy, focused ion beam, and high-resolution transmission electron microscopy. Clin Implant Dent Relat Res. 2008;10:11–22.

49. Kang BS, Sul YT, Oh SJ, Lee HJ, Albrektsson T. XPS, AES and SEM analysis of recent dental implants. Acta Biomater. 2009; 5:2222–9.

50. Roessler S, Zimmermann R, Scharnweber D, Werner C, Worch H. Characterization of oxide layers on Ti6Al4V and titanium by streaming potential and streaming current measurements. Colloids Surf B: Biointerfaces. 2002;26:387–95.

51. Cai K, Frant M, Bossert J, Hildebrand G, Liefeith K, Jandt KD. Surface functionalized titanium thin films: zeta-potential, protein adsorption and cell proliferation. Colloids Surf B: Biointerfaces. 2006;50:1–8.

52. Kim HM, Himeno T, Kawashita M, Lee JH, Kokubo T, Nakamura T. Surface potential change in bioactive titanium metal during the process of apatite formation in simulated body fluid. J Biomed Mater Res A. 2003;67:1305–9.

53. MacDonald DE, Deo N, Markovic B, Stranick M, Somasundaran P. Adsorption and dissolution behavior of human plasma fibronectin on thermally and chemically modified titanium dioxide particles. Biomaterials. 2002;23:1269–79.

54. Smith IO, Baumann MJ, McCabe LR. Electrostatic interactions as a predictor for osteoblast attachment to biomaterials. J Biomed Mater Res A. 2004;70:436–41.

55. Cooper JJ, Hunt JA. The significance of zeta potential in osteogenesis. Society for Biomaterials Annual Meeting. Pennsylvania, USA; 2006.

56. Nebe B, Finke B, Luthen F, Bergemann C, Schroder K, Rychly J, et al. Improved initial osteoblast functions on amino-functionalized titanium surfaces. Biomol Eng. 2007;24:447–54.

57. Larsson C, Esposito M, Liao H, Thomsen P. Titanium-bone interface in vivo. In: Brunette DM, Tengvall P, Textor M, Thomsen P, editors. Titanium in medicine. New York: Springer; 2001. p. 587–648.

58. Kalltorp M, Oblogina S, Jacobsson S, Karlsson A, Tengvall P, Thomsen P. In vivo cell recruitment, cytokine release and chemiluminescence response at gold, and thiol functionalized surfaces. Biomaterials. 1999;20:2123–37.

59. Jansson E, Kalltorp M, Thomsen P, Tengvall P. Ex vivo PMA-induced respiratory burst and TNF-alpha secretion elicited from inflammatory cells on machined and porous blood plasma clot-coated titanium. Biomaterials. 2002;23:2803–15.

60. Suska F, Esposito M, Gretzer C, Kalltorp M, Tengvall P, Thomsen P. IL-1alpha, IL-1beta and TNF-alpha secretion during in vivo/ex vivo cellular interactions with titanium and copper. Biomaterials. 2003;24:461–8.

61. Ma J, Ge J, Zhang S, Sun A, Shen J, Chen L, et al. Time course of myocardial stromal cell-derived factor 1 expression and beneficial effects of intravenously administered bone marrow stem cells in rats with experimental myocardial infarction. Basic Res Cardiol. 2005;100:217–23.

62. Cheng Z, Liu X, Ou L, Zhou X, Liu Y, Jia X, et al. Mobilization of mesenchymal stem cells by granulocyte colony-stimulating factor in rats with acute myocardial infarction. Cardiovasc Drugs Ther. 2008;22:363–71.

63. Wang Y, Deng Y, Zhou GQ. SDF-1alpha/CXCR4-mediated migration of systemically transplanted bone marrow stromal cells towards ischemic brain lesion in a rat model. Brain Res. 2008;1195:104–12.

64. Otsuru S, Tamai K, Yamazaki T, Yoshikawa H, Kaneda Y. Circulating bone marrow-derived osteoblast progenitor cells are

recruited to the bone-forming site by the CXCR4/stromal cell-derived factor-1 pathway. Stem Cells. 2008;26:223–34.

65. Son BR, Marquez-Curtis LA, Kucia M, Wysoczynski M, Turner AR, Ratajczak J, et al. Migration of bone marrow and cord blood mesenchymal stem cells in vitro is regulated by stromal-derived factor-1-CXCR4 and hepatocyte growth factor-c-met axes and involves matrix metalloproteinases. Stem Cells. 2006;24:1254–64.

66. Furze RC, Rankin SM. Neutrophil mobilization and clearance in the bone marrow. Immunology. 2008;125:281–8.

67. Nagase H, Miyamasu M, Yamaguchi M, Imanishi M, Tsuno NH, Matsushima K, et al. Cytokine-mediated regulation of CXCR4 expression in human neutrophils. J Leukoc Biol. 2002;71:711–7.

68. Martin C, Burdon PC, Bridger G, Gutierrez-Ramos JC, Williams TJ, Rankin M. Chemokines acting via CXCR2 and CXCR4 control the release of neutrophils from the bone marrow and their return following senescence. Immunity. 2003;19:583–93.

69. Boyan BD, Schwartz Z. Response of musculoskeletal cells to biomaterials. J Am Acad Orthop Surg. 2006;14:S157–62.

70. Gronthos S, Simmons PJ, Graves SE, Robey PG. Integrin-mediated interactions between human bone marrow stromal precursor cells and the extracellular matrix. Bone. 2001;28:174–81.

71. Gronowicz G, McCarthy MB. Response of human osteoblasts to implant materials: integrin-mediated adhesion. J Orthop Res. 1996;14:878–87.

72. Setzer B, Bachle M, Metzger MC, Kohal R. J. The gene-expression and phenotypic response of hFOB 1.19 osteoblasts to surface-modified titanium and zirconia. Biomaterials. 2009;30:979–90.

73. Ogawa T, Nishimura I. Different bone integration profiles of turned and acid etched implants associated with modulated expression of extracellular matrix genes. Int J Oral Maxillofac Implants. 2003;18:200–10.

74. Ozawa S, Ogawa T, Iida K, Sukotjo C, Hasegawa H, Nishimura RD, et al. Ovariectomy hinders the early stage of bone-implant integration: histomorphometric, biomechanical, and molecular analyses. Bone. 2002;30:137–43.

75. Hughes DE, Salter DM, Dedhar S, Simpson R. Integrin expression in human bone. J Bone Miner Res. 1993;8:527–33.